The effect of adding ethanol on the ignition properties of fast pyrolysis bio oils

R. Calabria[1], F. Chiariello[1], P. Massoli[1], A. Frassoldati[2], B. van de Beld[3], , R.T.E. Hermanns[4], A. Oasmaa[5], A. Toussaint[6]

1 Istituto Motori, CNR, Napoli, Italy
2 Politecnico di Milano, Italy
3 BTG Biomass Technology Group B.V, The Netherlands
4 OWI Oel-Waerme-Institut gGmbH, Germany
5 VTT Technical Research Centre of Finland Ltd.
6 BTG BioLiquids B.V.

Abstract

In this paper, the ignition behaviour of droplets composed by crude FPBO and FPBO/EtOH blends at normal pressure is discussed. The tests were carried out, in a closed single droplet combustion chamber with optical accesses, on droplets of diameter in the range 0.8 mm -1.4 mm. FPBO/EtOH blends with percentage of alcohol varying between 5 % v/v and 50 % v/v were tested. To analyse the effectiveness of the addition of ethanol on the ignition properties of FPBOs, the study was also carried out on the crude FPBO used to form the blends. 1D modelling of the evaporation and ignition of droplets of crude FPBO and blends FPBO/EtOH is also discussed. The comparison of numerical and experimental results shows that the model is able to capture the main features of the heating phase of the complex fuels forming the droplets.

Introduction

The utilization of renewable energy and the substitution of the fossil fuels by alternative sources is one of the priority points for a sustainable development. Fuels obtained from biomasses can become a valid alternative to displace fossil fuels, also in the light of stricter environmental constraints. In the outline of alternative liquid fuels, pyrolysis oils obtained from the pyrolysis of biomasses represent an interesting topic as concerns their use in power plants and engines for stationary applications. Fast pyrolysis oils from biomasses (FPBO) are black-brownish liquids characterized by peculiar properties and composition. Their typical features are high viscosity (10-200 cSt @ 40 °C), acidity (pH 2-3) and density (1.2 kg/dm3 @ 40 °C). Water represents one of their majority components (16%-30%) and it is inherently dispersed in the oil. The elemental composition of FPBOs is, in average, C 50–70%, N 0–1%, H 4–10%, O 25–40%. The high content of oxygen (water and oxygenated compounds) is responsible for the low heating value of POs that typically ranges between 15 MJ/kg and 20 MJ/kg.
The composition and the properties of the fast pyrolysis bio-oils depend on the origin feedstock as well as the conditions of production and storage. The peculiar composition of FPBOs and the tendency to phase separation and polymerization require the systematic study of the most suitable procedures for their handling and storage as well as technical solutions for the use in the commercial combustion systems. A viable solution to reduce viscosity and acidity and to improve the stability of POs is represented by the mixing with oxygenated compounds. The addition of alcohols and/or water results in a decrease of viscosity and acidity. The utilization of such compounds characterized by a low boiling point is also favourable for improving secondary atomization. Typically, the addition of alcohols is recommended for increasing the stability of FPBOs. However, the scarce autoignition properties of alcohols has to be take into account for utilization of FPBOs blends in engines, unless cetane improvers are used. The influence of ethanol is significant also in the case of burners due to the clear benefits on atomisation generated by the reduction of viscosity and combustion quality. However, a cost/benefit analysis concerning economical as well as safety and handling issues would

indicate a limited concentration of alcohol. Thus, the analysis of the influence of ethanol (EtOH) on the ignition properties of FPBOs is an issue that should be carefully addressed.
In this paper, the ignition behaviour of droplets composed by crude FPBO and FPBO/EtOH blends at normal pressure is discussed. The ignition experiments were carried out in a closed single droplet combustion chamber with optical accesses. Droplets of FPBO/EtOH blends were suspended to bare thermocouple junctions (ϕ = 75 μm). The thermocouple provided the temperature of droplets during the different phases of droplet evolution. A high speed digital imaging systems (Photron SAX2, max acquisition rates of 1 Mframes per second) was used to follow the phenomenology exhibited by the droplets before and after the ignition, as well as the variation of their size. The ignition time is determined by combining the analysis of the high speed imaging, the droplet temperature and the temperature of the environment around the droplet, measured by a second thermocouple placed laterally to the central one used to suspend the droplet. The tests were carried out on droplets of 0.8 mm -1.4 mm of FPBO/EtOH blends with percentage of alcohol varying between 5 % v/v and 50 % v/v. To analyse the effectiveness of the addition of ethanol on the ignition properties of FPBOs, the study was also carried out on the crude FPBO used to form the blends.

Ignition Time

In combustion science, the definition of the ignition time or, in equivalent way, the induction time, varies considerably throughout the literature. The concept of induction time presupposes that the reactants will have a well-defined period of nearly isothermal reaction followed by a very rapid exothermal event (ignition). The end of the induction period is typically marked by a sharp increase in pressure, temperature, and product species. This supposition is reasonable for most cases because almost all combustion reactions initially consist of thermally-neutral, chain-branching processes that create the intermediate and radical species that ultimately combine to form products. The question arises of exactly how to define it. The definition is not important if all variables (temperature, pressure, reactant, product and species concentrations) change rapidly at the same time [1]. The chemical reactions involved in ignition are also characterised by significant chemiluminescence. Hence, one of the typical experimental approaches used for defining the ignition instant is based on the measure of the luminosity.
In our study, the ignition time is defined as the instant in which a strong temperature discontinuity or significant increases of luminosity occur in the region around the droplet. It is determined by a thermo-optical investigation that combines high speed imaging analysis, to catch the luminosity of the flame, and the measure of the temperatures of the droplet and the environment close to the droplet. Typically, when ignition takes place, a marked increase of the droplet surrounding atmosphere temperature occurs, because the exothermal event (combustion), together to a luminous signal.
The ignition delay can be schematically divided into two parts: the physical delay and chemical delay. In a droplet, the physical processes occurring in the first period are the heating of the liquid fuel, the vaporization of the fuel droplets and the mixing of the fuel vapour with the air. The chemical delay is the time necessary to establish the optimal conditions of the fuel vapour/air mixture to start oxidation process. In practical combustion systems, the ignition delay generally takes into account also the pre-combustion reactions of the fuel, air, residual gas mixture which lead to autoignition. [2,3,4].
Viscosity of the fuel governs the physical delay of fuel combustion process in fuel sprays. The quality of the fuel atomization in a combustion system is strictly related to the Sauter Mean Diameter (SMD) of the droplets after injection. For either airblast and pressure swirler atomizers, the SMD is dependent of fuel viscosity [5]. The evaporation rate is inversely proportional to the square of SMD. This point reflects the fact that to higher viscosity values, typical of FPBO, correspond higher ignition time and lower combustion efficiency [6].

FPBO are non-flammable, non-distillable, high viscosity fuel and possess only limited volatility, due to the very high heat of vaporization of water included in the fuel [7]. Dilution of FPBO with ethanol (EtOH) is a well know practice to reduce considerably the fuel viscosity. As reported in literature the viscosity of the FPBO/EtOH blends at 20% in alcohol is reduced more than half. Yet, the blends preserve the strong dependence of the viscosity by liquid temperature as the FPBO [8]. EtOH addition also improves the volatility of the fuel, creating benefits for the fuel vapour/air mixture ignition and for the stability of the flame in the mixing-controlled combustion phase, where the lean blow-out limit is not only governed by the heat released into the vapour mixture but also by the time required to vaporize fuel droplets [5, 8].
In FPBO combustion, NOx emissions are mainly governed by the nitrogen content in the fuel and, so, it is related to the FPBO feedstock. The low heating value of FPBO due to the high water content and the consequentially low adiabatic flame temperature is the evidence that no thermal NO_X are produced (according the Zeldovich mechanism) when bio-oil is used as fuel [9].
Blending EtOH to FPBO affects the CO production in the way that a higher fuel heating value due to the presence of the alcohol reduces the fuel flow consumption at the same chemical power input in the combustion system. Being CO an intermediate in the oxidation process of the C-based fuels, the emission is governed exclusively by the kinetics and by the combustor efficiency [9].
Yet, regarding the particulate emissions in combustion systems, adding ethanol to FPBO increases the particles production in the nucleation mode for diameters less than 50 nm and decreases more than 80% the total amount in the accumulation mode with larger diameters of 50-1000 nm, where soot is actually produced, due to the high oxygen content in the fuel [10]. According other authors, although the measured particulate matter (PM) emitted by the combustion of wood FPBO consists of both cenospheric residues and inorganic matter, the majority is composed of ash [11].

Experimental apparatus

The ignition experiments were carried out in the combustion cell for single droplet depicted in Fig. 1. A thin (75 µm wires) bare thermocouple placed at the centre of the cell was used to hang and measure the temperature of the droplets. A CMOS high-speed camera (Photron Fastcam SA-X2, max acquisition rates of 1 Mframes per second, 1024x1024 pixels, 12-bit) was used to visualize the complex phenomenology exhibited by droplets before and after the ignition, as well as the variation of their size. The acquisition frequency was set at 1,000 frames/sec and full frame resolution. All the signals were acquired by a LeCroy Waverunner 104MXI-A transient recorder. The heating of droplets was obtained by a resistive coil placed below the droplets (Fig.1, bottom). In each experiments, the test is repeated with and without the droplet suspended on the thermocouple, to measure the heating rate capability of the system. Then the experiment is repeated and in this case the thermocouple measures the temporal evolution of the liquid droplet.

The ignition time is determined by combining the analysis of the high speed imaging, the temperature of the droplet and the temperature of the environment close to the droplet, measured by a second thermocouple placed laterally to the central one (Fig.1, left). When ignition takes place, the lateral thermocouple shows a marked increase of the sensed temperature because exposed to the flame that is developing and standing around the droplet. This second thermocouple is fundamental in the analysis of the ignition of droplets because for light and oxygenated compounds, as the alcohol in the mixtures, the initial flame can be so feeble that its settling can be not clearly revealed by optical visualization. Obviously, the ignition is sensed by the central thermocouple too but its signal is lower and can be delayed because it is shielded by the liquid droplet.

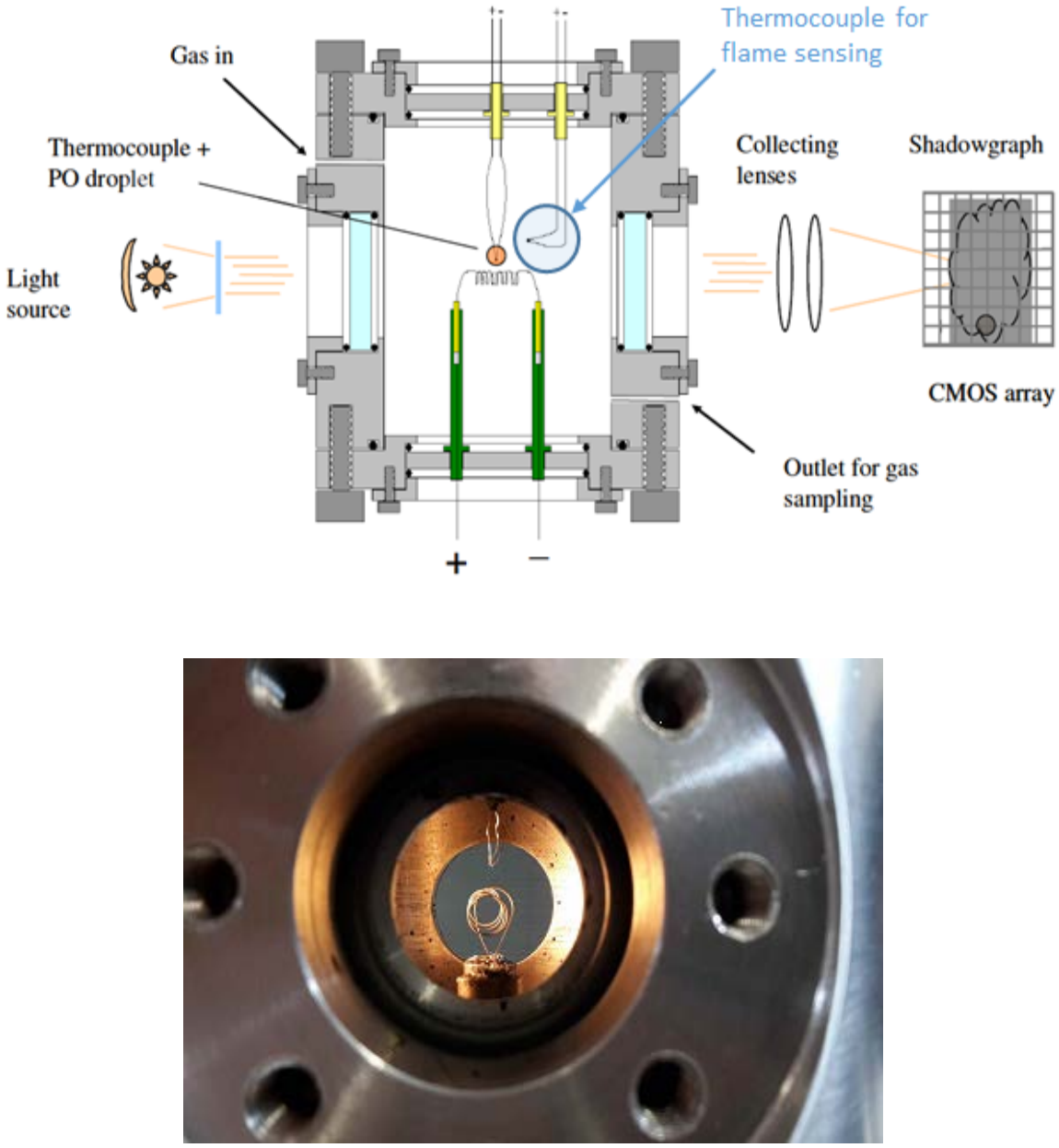

Figure 1: Experimental set-up (top: combustion cell layout; bottom: side view of the group coil/thermocouples inside the cell)

Experimental Results

The experimental activities regarded droplets in the range 0.8 mm – 1.3 mm of a crude FPBO and FPBO/ethanol blends at various alcohol content in the range 5%-50%. Specifically, they were tested blends with 50%, 20%, 10%, 5% ethanol in volume to fuel.

As an example, in Figure 2 they are reported the temperature (right) and the projected area (left) of droplets of FPBO and FPBO/EtOH 50% v/v, as determined by the central thermocouple signal and analysis of the images in the high speed movies, respectively. The dashed bars represent, in order, the ignition time and the end of the heterogeneous combustion (the combustion of the solid carbonaceous). The marked swelling of the droplets is shown through the considerable oscillations that characterize the curve of the projected areas. In particular the FPBO droplet shows swelling

values up to almost four times the initial projected area. One of the most relevant feature is the net difference between the ignition time of crude oil and the blend. In these two tests, the ignition time of the blend droplet is almost the half that of the FPBO droplet.

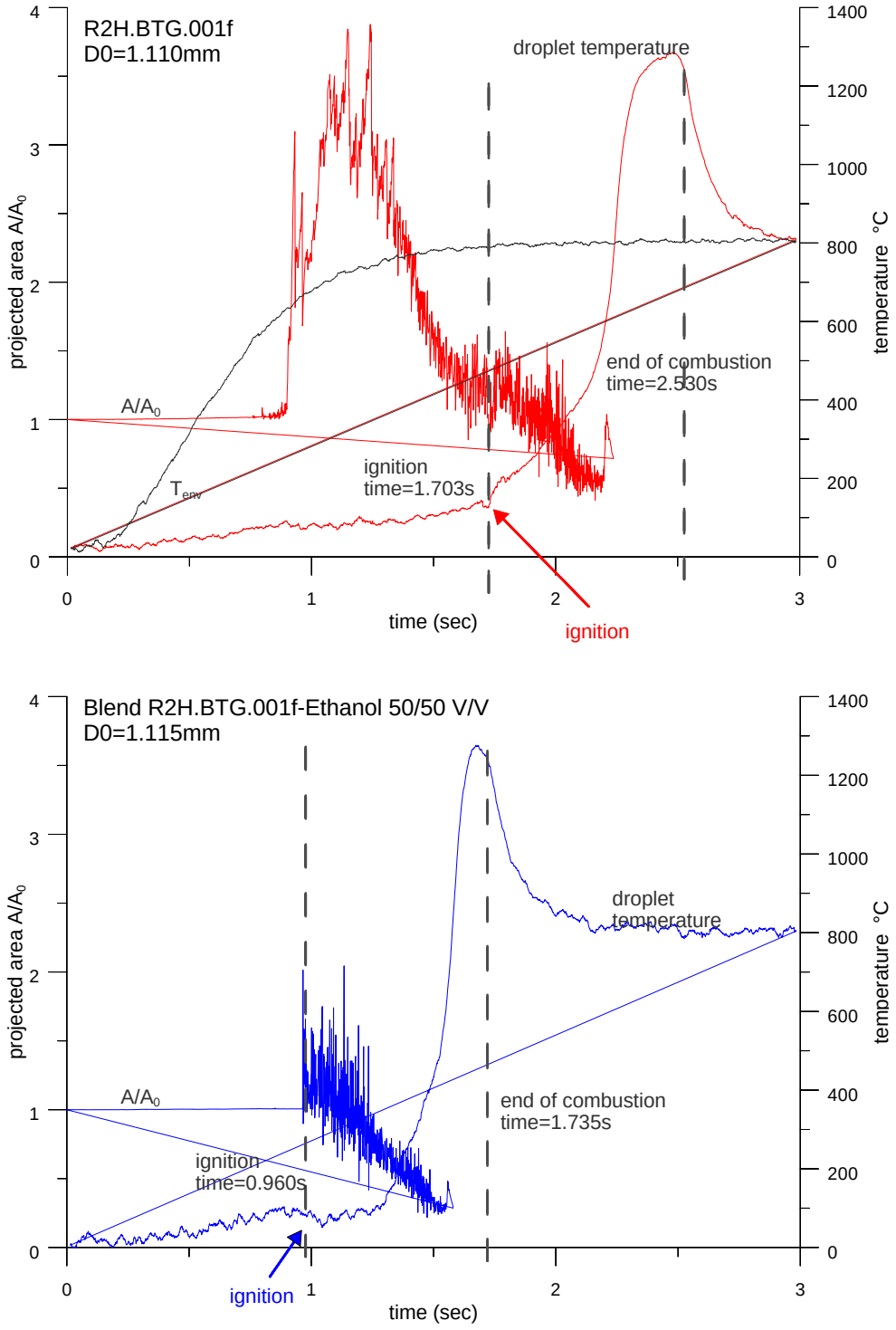

Figure 2: Combustion behaviour of droplets of crude FPBO (top) and mix FPBO/EtOH 50/50 v/v (bottom)

The analysis of the high speed movies showed that all droplets exhibited marked swelling associated to sputtering (ejection of liquid matter) and puffing (ejection of vapour puffs) before and after ignition. In Figure 3 is reported a sequence of images showing the microexplosive character of a FPBO/EtOH 50/50 v/v droplet.

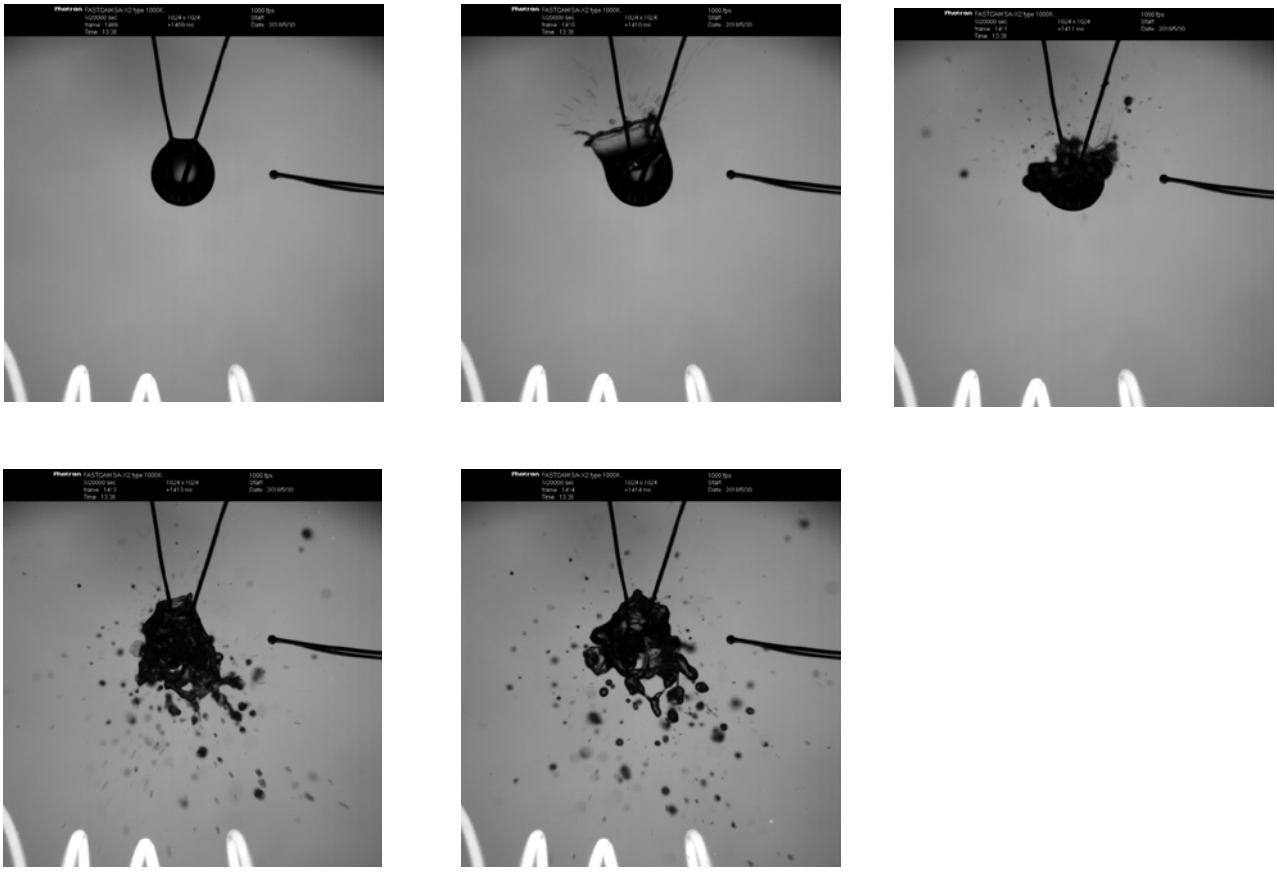

Figure. 3 Microexplosion behavior of FPBO/EtOH 50/50 v/v droplet

Figure 4 shows the ignition time, t_{ign}, for the different samples as a function of the initial droplet diameters D_0. While at 50% of alcohol, experimental data show a trend of the ignition time with the initial droplet diameter similar to FPBO, interesting enough, the dependence of t_{ign} on D_0 decreases with the percentage of alcohol and becomes practically flat for a concentration of alcohol of 10% or lesser.

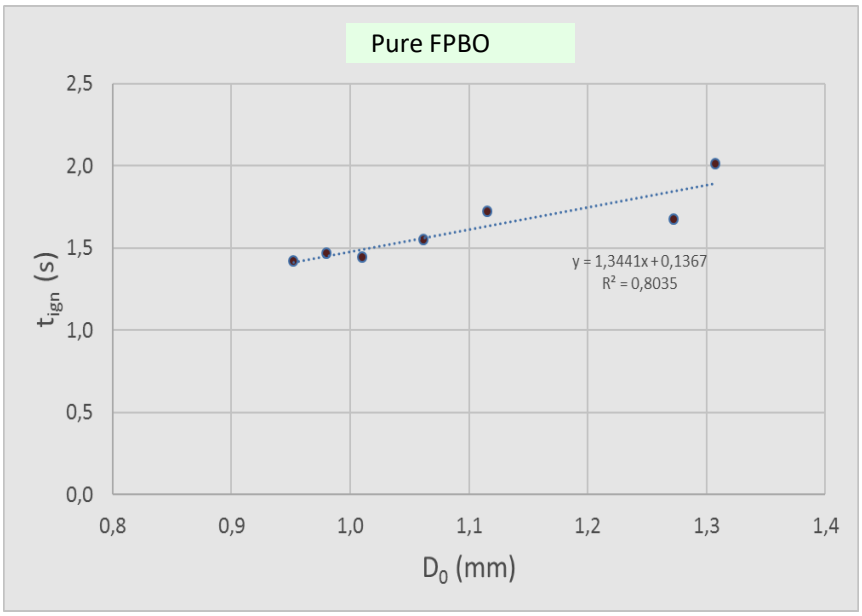

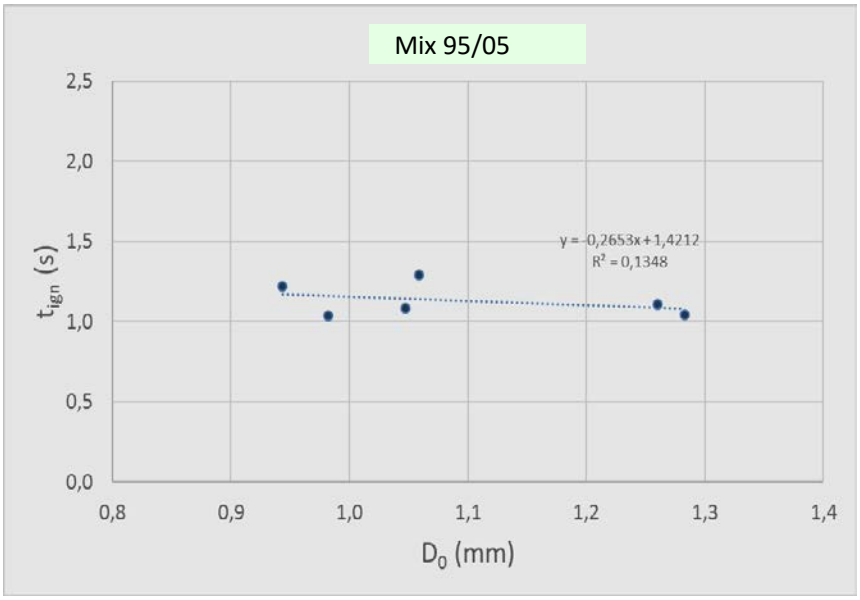
Mix 95/05
y = -0,2653x + 1,4212
R² = 0,1348
t_ign (s)
D_0 (mm)
2,5
2,0
1,5
1,0
0,5
0,0
0,8
0,9
1,0
1,1
1,2
1,3
1,4

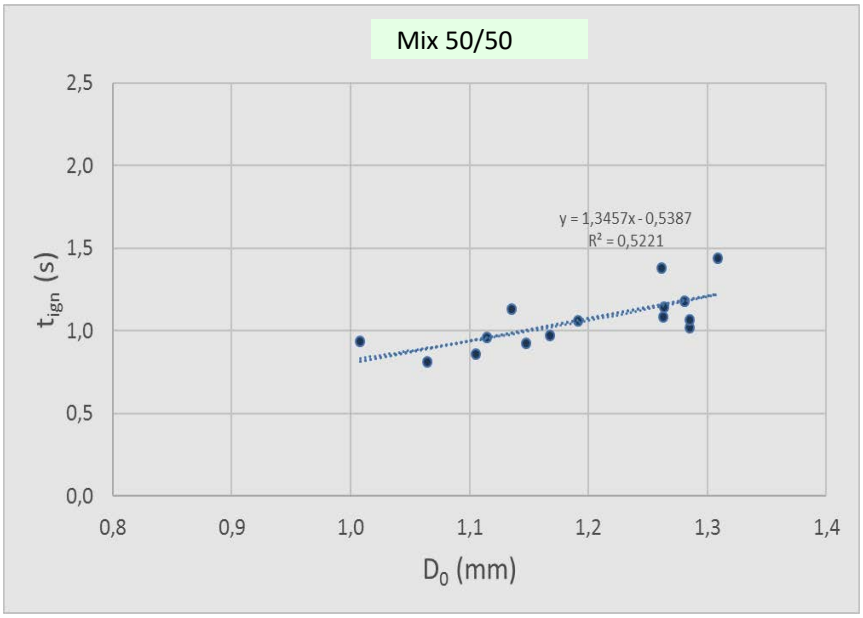
Mix 50/50
y = 1,3457x - 0,5387
R² = 0,5221
t_ign (s)
D_0 (mm)
2,5
2,0
1,5
1,0
0,5
0,0
0,8
0,9
1,0
1,1
1,2
1,3
1,4

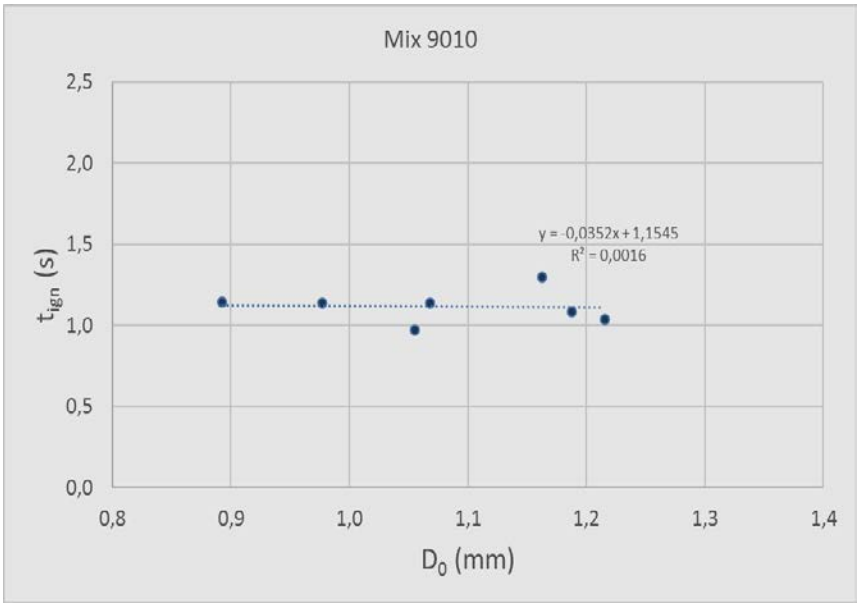
Mix 9010
y = -0,0352x + 1,1545
R² = 0,0016
t_ign (s)
D_0 (mm)
2,5
2,0
1,5
1,0
0,5
0,0
0,8
0,9
1,0
1,1
1,2
1,3
1,4

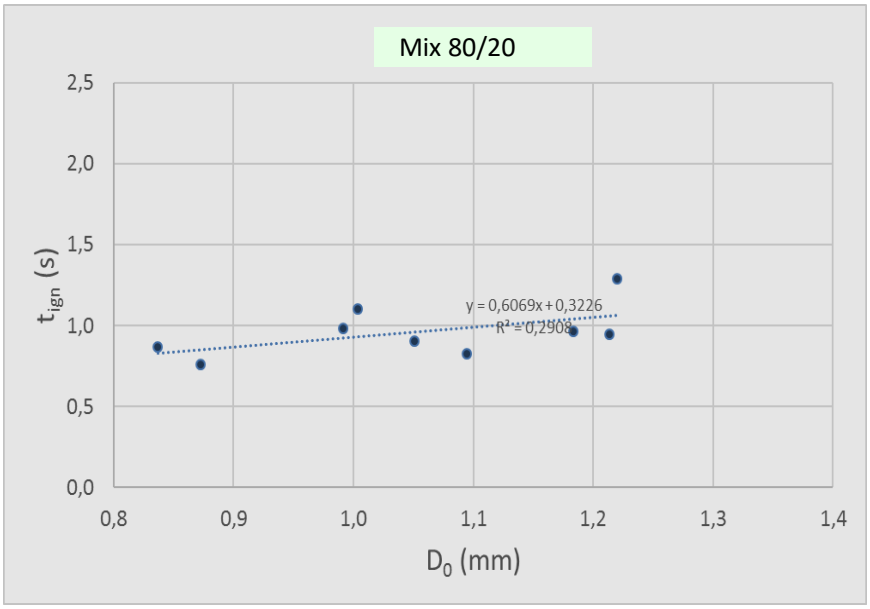

Figure 4: Ignition time with respect to the droplet diameter of the reference crude FPBO and the various FPBO/EtOH mixtures

Droplet evaporation 1D model

In this section, the heating of spherical droplets in 1D geometry is briefly summarized. In this model the following assumptions are made:

- Spherically symmetric droplet;
- Constant pressure;
- Equilibrium conditions at the liquid/gas interface.

Conservation of species, energy and velocity in the droplet in the liquid phase is thus solved with the following set of equations [12]:

$$\rho_L\left(\frac{\partial Y_{i,L}}{\partial t}+v_L\frac{\partial Y_{i,L}}{\partial r}\right)=-\frac{1}{r^2}\frac{\partial}{\partial r}\left(r^2 j_{L,i}\right) \quad (1)$$

$$\rho_L c_L\left(\frac{\partial T_L}{\partial t}+v_L\frac{\partial T_L}{\partial r}\right)=-\frac{1}{r^2}\frac{\partial}{\partial r}\left(r^2 k_L\frac{\partial T_L}{\partial r}\right)-\sum_i j_{L,i}c_{L,i}\frac{\partial T_L}{\partial r} \quad (2)$$

$$\frac{\partial \rho_L}{\partial t}+\frac{1}{r^2}\frac{\partial}{\partial r}\left(r^2\rho_L v_L\right)=0 \quad (3)$$

where the subscript L refers to liquid-phase properties. ρ is the density, v is the convective velocity, Y_i is the mass fraction of the *i*-th species, r is the radial coordinate, j is the diffusion flux, k is the thermal conductivity. $c_{L,i}$ and c_L are, respectively, the heat capacity of the *i*-th species and of the mixture. The diffusion fluxes are described through the Stefan-Maxwell theory [13].

Boundary conditions at the droplet centre require zero velocity for the liquid, and homogeneous Neumann conditions are prescribed for temperature and mass fractions. Interface properties are calculated from thermodynamic equilibrium and mass and energy flux continuity.

Similar equations are obtained for the gas phase, although further contributions must be included:

$$\rho_G\left(\frac{\partial Y_{i,G}}{\partial t}+v_G\frac{\partial Y_{i,G}}{\partial r}\right)=-\frac{1}{r^2}\frac{\partial}{\partial r}\left(r^2\left(j_{G,i}+j_{th,i}+j_{soret,i}\right)\right)+\dot{\Omega}_{G,i}\qquad i=1\dots NS \tag{4}$$

$$\rho_G c_G\left(\frac{\partial T_G}{\partial t}+v_G\frac{\partial T_G}{\partial r}\right)=-\frac{1}{r^2}\frac{\partial}{\partial r}\left(r^2 k_G\frac{\partial T_G}{\partial r}\right)-\sum_i j_{G,i}c_{G,i}\frac{\partial T_G}{\partial r}-\sum_{i=1}^{NS}\dot{\Omega}_{G,i}\hat{h}_{R,i}-\nabla q_R \tag{5}$$

$$\frac{\partial \rho_G}{\partial t}+\frac{1}{r^2}\frac{\partial}{\partial r}(r^2\rho_G v_G)=0 \tag{6}$$

where the subscript G indicates gas-phase properties. With reference to the *i*th gas-phase species, Y_i is its mass fraction, $j_{G,i}$ is its diffusion flux, calculated according to the Fick's law, $j_{th,i}$ is the flux due to thermophoresis, $j_{soret,i}$ is the flux generated by the Soret effect, $\dot{\Omega}_{G,i}$ is its formation rate, i.e. $\dot{\Omega}_{G,i}=\sum_{j=1}^{NR}\nu_{ij}r_j$, where r_j is the *j*-th reaction rate. NS and NR are the total number of species and reactions. $\hat{h}_{R,i}$ is the mass enthalpy of formation of the *i*-th species and q_R is the radiative heat flux.
The resulting set of equations is discretized using an adaptive grid, more refined in proximity of the interface from the liquid side, as well as in the whole flame region in the gas phase. Further details on this model are available in the literature [12,14,15].
This 1D droplet model described has been adopted to predict the experimental measurements performed on suspended droplets. It is important to underline that the 1D model cannot account explicitly for buoyancy because of the assumption of spherical symmetry. In the experiments, the droplet is heated by a heating coil, which is placed below the droplet. This device is modelled using the 1D approach by assigning the measured time evolution of the temperature, experienced by the thermocouple (during the experimental test without a suspended droplet) as a boundary condition for the gas phase computational domain surrounding the droplet. As a consequence of this imposed increasing temperature at the boundary, the gas phase also increases its temperature due to the radial diffusion of heat. In this way, the heated gas reaches the liquid droplet boundary and the evaporation begins. However, as a consequence of this simplification, there is a delay in the numerical computations due to the time needed for the heat diffusion in the gas phase. Therefore, in order to compare model predictions and experimental measurements it is necessary to apply an arbitrary time shift. For the computational domain used in this example, made of 1000 grid points for the gas phase which extends up to a maximum radial distance equal to ~20 initial droplet radii, the required time shift is relatively small (0.2 [s]). Furthermore, since in the experiments a significant velocity is observed due to the effect of buoyancy induced by the heating coil placed below the suspended droplet, a correction is required to take into account the enhanced heat transfer from the gas phase to the droplet (the 1D model would only consider conduction of heat in the quiescent gas phase). On the contrary, a convective velocity of ~40 cm/s is present around the droplet. Thus, the additional convective heat flux is calculated using a heat transfer coefficient and the difference in temperature between the gas phase (maximum) temperature and the droplet surface temperature:

$$Q_{convective}=h_{convective}\cdot\Delta T \tag{7}$$

The heat transfer coefficient is evaluated on the basis of a Nusselt number, the thermal conductivity at the droplet's surface and the droplet diameter (D).

$$h_{convective}=Nu\cdot\frac{kg}{D} \tag{8}$$

$$Nu=2+0.60\cdot \mathrm{Re}^{1/2}\cdot\ \mathrm{Pr}^{1/3} \tag{9}$$

Reynolds and Prandtl numbers are evaluated using the instantaneous droplet diameter, the corresponding physical properties at the droplet surface and the convective velocity.

Figure 5 shows the predicted temperature of droplets of FPBO (top) and the blend FPBO/EtOH 50/50 (bottom). In the simulation, they have been assigned the experimental initial diameter of the droplets (1.110 mm for FPBO and 1.115 mm for Mix 50/50, respectively) and the environment temperature as experimentally measured (T_{env} in Fig. 2).

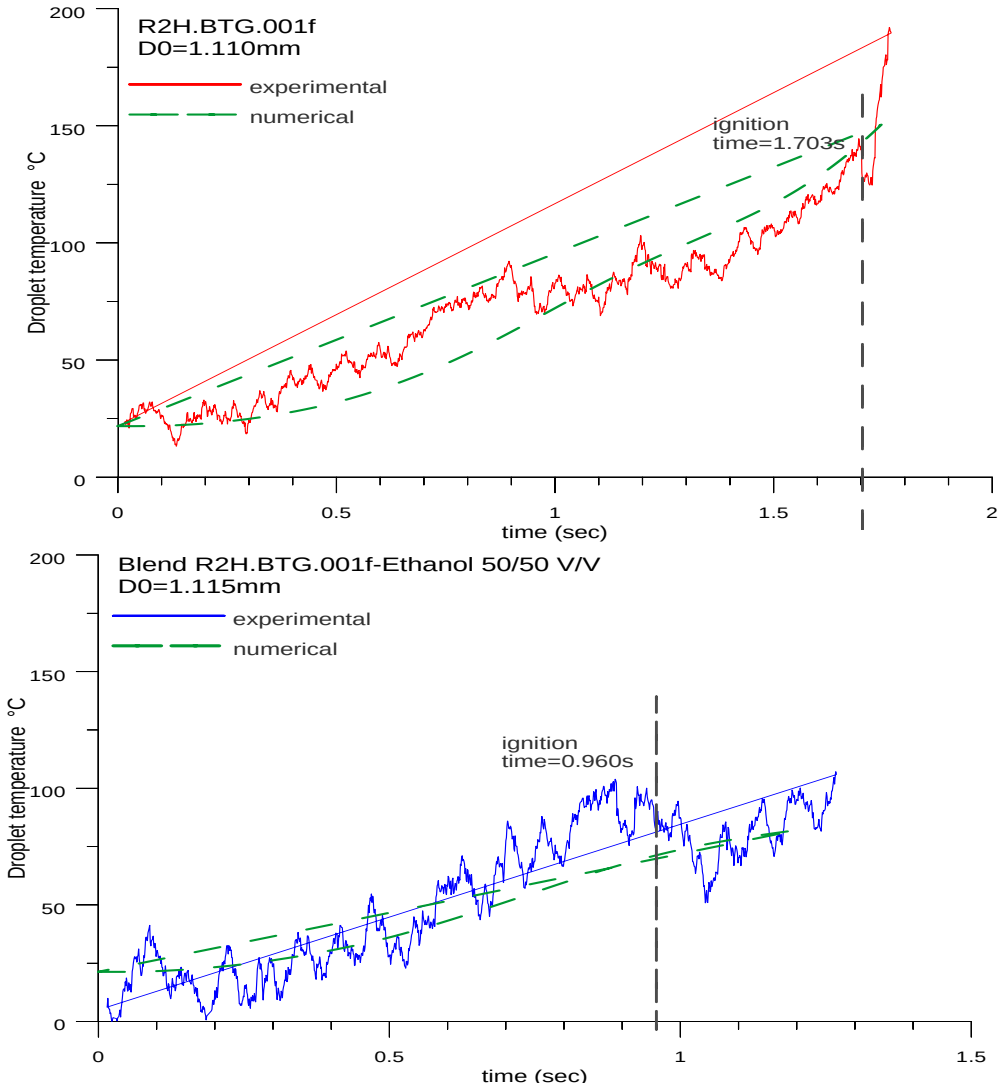

Figure 5 – Temperature of droplets of FPBO crude oil (top) and mixture 50/50 FPBO/EtOH (bottom). Experimental data (continuous line) and numerical 1D model predictions (dashed line).

Final Remarks

Figure 6 reports the averaged value of the ignition times for the crude oil and the mixtures. For each fuel sample, the blue rhombus represents the average of the diameters of droplets were tested while the violet one is the average of the values of tign measured on all the droplets of that sample. With squared symbols, they are also reported the standard deviations of the droplets diameters and ignition times. As described by the values of mean diameters and their standard deviations, the tests were carried out on sets of droplets homogeneous enough.

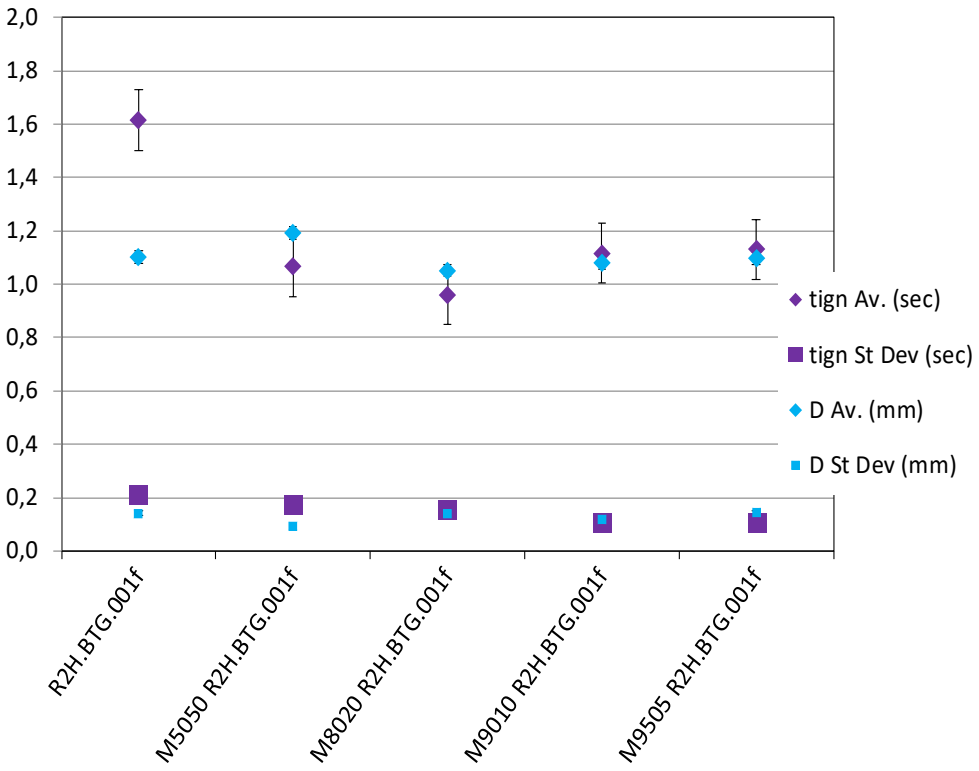

Figure 6 – Average value of the ignition times with respect to the average of the diameters of the droplets for the reference crude FPBO and the blends with ethanol (from left to right with decreasing ethanol concentration). The standard deviation of the average of the two parameters is also reported.

From a practical point of view, the most relevant finding can be inferred by Fig.5 is the noticeable reduction of the ignition time of FPBO/EtOH blends: it is around 1.6 s for the crude oil and 1.1 s for all the blends. Very interesting, the decrease of the ignition time is identical for all alcohol concentrations, being the oscillation of the values for the different blends within the experimental uncertainty. This means that tign is insensitive to the concentration of ethanol and, hence, the improvement of the ignition properties of a FPBO can be gained with low concentration of alcohol.
Concerning the 1D modelling, notwithstanding the significant simplifications imposed concerning the absence of buoyancy and the spherical symmetry, the model is able to capture the main features of the heating phase of the complex fuels forming the droplets, as it is possible to appreciate in Fig.5.

Acknowledgement

The Residue2Heat project has received funding from the European Union's Horizon 2020 Research and Innovation programme under Grant Agreement No. 654650.

References

[1] R. Akbar, M. Kaneshige, E. Schultz, J. Shepherd, Detonations in H2-N2O-CH4-NH3-O2-N2 Mixtures, Graduate Aeronautical Laboratories California Institute of Technology, Pasadena, CA, Explosion Dynamics Laboratory Report FM97-3July 24, (1997), Revised January 17, 2000Prepared for Los Alamos National Laboratory under Contract 929Q0015-3A, DOE W-7405-ENG-36.

[2] J.B. Heywood, Internal Combustion Engine Fundamentals, Mc-Graw Hill Book Company, New York (1988)

[3] F. Z. Sánchez, C. V. M. Braga, L. C. Braga, S. L. Braga, F. G. Dias, F. Y. Turkovics, R. N. C. De Souza, Experimental Study of the Ignition Delay for Ethanol-Powered in a Rapid Compression Machine, SAE Technical Paper 2014-36-0127, (2014) , https://doi.org/10.4271/2014-36-0127.

[4] M. Shahabuddin, A.M. Liaquat, H.H. Masjuki, M.A. Kalam, M. Mofijur, Ignition delay, combustion and emission characteristics of diesel engine fueled with biodiesel, Renewable and Sustainable Energy Reviews 21 (2013) 623–632.

[5] AH. Lefebvre, Atomization of alternative fuels, AGARD CP-422, (1988).

[6] G. López Juste, J.J. Salvá Monfort, Preliminary test on combustion of wood derived fast pyrolysis oils in a gas turbine combustor, Biomass and Bioenergy 19 (2000) 119±128.

[7] J. Lehto, A. Oasmaa, Y. Solantausta, M.i Kytö, D. Chiaramonti, Review of fuel oil quality and combustion of fast pyrolysis bio-oils from lignocellulosic biomass, Applied Energy 116 (2014) 178–190.

[8] T. Tzanetakis, N. Farra, S. Moloodi, W. Lamont, A. McGrath and M. J. Thomson, Spray Combustion Characteristics and Gaseous Emissions of a Wood Derived Fast Pyrolysis Liquid-Ethanol Blend in a Pilot Stabilized Swirl Burner, Energy Fuels 2010, 24, 5331–5348: DOI:10.1021/ef100670z.

[9] J. A. Martin, A. A. Boateng, Combustion performance of pyrolysis oil/ethanol blends in a residential-scale oil-fired boiler, Fuel 133 (2014) 34–44.

[10] S. Lee, Y. Jang, T. Y. Kim, K.Yong Kang, H. Kim and Jonghan Lim, Performance and Emission Characteristics of a Diesel Engine Fueled with Pyrolysis Oil-Ethanol Blend with Diesel and Biodiesel Pilot Injection, SAE Int. J. Fuels Lubr. 6(3):785-793, (2013), doi:10.4271/2013-01-2671.

[11] T. Tzanetakis, S. Moloodi, N. Farra, B. Nguyen, M. J. Thomson, Spray Combustion and Particulate Matter Emissions of a Wood Derived Fast Pyrolysis Liquid-Ethanol Blend in a Pilot Stabilized Swirl Burner, Energy Fuels 20112541405-1422, (2011), doi:10.1021/ef101500f.

[12] A. Cuoci, M. Mehl, G. Buzzi-Ferraris, T. Faravelli, D. Manca, E. Ranzi, Autoignition and burning rates of fuel droplets under microgravity, Combustion and Flame 143 (2005) 211-226.

[13] R. Taylor, R. Krishna, Multicomponent mass transfer, John Wiley & Sons, 1993.

[14] A. Stagni, L. Esclapez, P. Govindaraju, A. Cuoci, T. Faravelli, M. Ihme, The role of preferential evaporation on the ignition of multicomponent fuels in a homogeneous spray/air mixture, Proceedings of the Combustion Institute, Volume 36, Issue 2, (2017) 2483-2491.

[15] A. Stagni, A. Cuoci, A. Frassoldati, E. Ranzi, T. Faravelli, Numerical investigation of soot formation from microgravity droplet combustion using heterogeneous chemistry, Combustion and Flame, Volume 189, (2018) 393-406